Laser Processing High Aspect Ratio Groove Wick for Improving the Thermal Performance of Flat Micro Heat Pipe

X. Z. Xie[1,2], W. J. Hong[1], J.Y. Long[1], X. Wei[1], W. Hu[1], Q.L. Ren[1]

[1]*Laser Micro/Nano Processing Research Lab, School of Electromechanical Engineering, Guangdong University of Technology, Guangzhou 510006, P.R. China*
[2]*Department of Experimental Teaching, Guangdong University of Technology, Guangzhou 510006, P.R. China*
E-mail: xiaozhuxie@gdut.edu.cn and longjy@gdut.edu.cn

Groove wick micro heat pipes are characterized by light weight, fast thermal response and high permeability which are in line with the current trend of lightweight electronic devices. As an efficient heat transfer device, flat micro heat pipes (FMHP) have been widely used for thermal management of electronic devices because of their excellent thermal performance and high reliability. In this paper, FMHP with microgrooves wick was processed on the copper substrate by 1064nm pulsed fiber laser. The influence of various laser processing parameters including pulse duration, scanning speed, scanning interval and the number of scanning cycles on the size and morphology of groove structures have been studied. The grooves with different aspect ratio are obtained by changing the number of scanning cycles, and the effects of aspect ratio on the droplet flow velocity are investigated respectively. Experimental results indicate that grooves with larger aspect ratio exhibits greater capillary pressure which leads to a faster droplet flow velocity. Groove wick with the aspect ratio of 2.5 whose average groove depth of 125 μm and groove width of 50 μm is fabricated successfully, and the FMHP with the groove wick of this type have the best heat transfer property.
DOI: 10.2961/jlmn.2019.01.0011
Keywords: pulsed fiber laser; copper; groove structure; surface morphology; processing parameters

1. Introduction

Recently, with the rapid development of microelectronics technology and the information industry, high power and highly integrated electronic chips generate more heat and create a challenge for heat dissipation and cooling, corresponding thermal management systems are urgently required [1-3]. As an efficient heat transfer device, flat micro heat pipes (FMHP) have been widely used for thermal management of electronic devices because of their excellent thermal performance and high reliability.

The thermal performance of the FMHP depends mainly on the capillary structure, lots of experimental and theoretical work have been published on flat heat pipes with different inner capillary structures, such as sintered powder wicks [4, 5], screen meshes [6, 7], grooves [8, 9] and composite wick [10]. The main features of groove wick heat pipe are light weight, fast thermal response, and high permeability, which is in line with the trend of light and thin electronic devices. Current methods to process the groove wick are chemical etching, electro-discharge machining (EDM), extrusion–ploughing [11, 12] and laser processing [13, 14]. Compared with other processing methods, laser processing is simple, flexible and high machining precision, it is particularly suitable for processing grooves wick. But weak capillary force due to the groove wick structure can be a shortcoming. Several studies were conducted to optimize the grooves of the heat pipe to overcome the weak capillary force. For instance, Li Xibing et al. [15] established several mathematical models for theoretical analysis, and finally experiments were conducted on micro heat pipes of different groove structures manufactured by high speed spinning. The results showed that a micro heat pipe with trapezium-grooved wick has fairly good warm starting performance. That is, the heat pipe can enter from the non-working state to the working state more quickly, and its inclination angle greatly influences heat transfer performance. C. Wang et al. [16] presented two different flat plate heat pipes. The capillary structure is made of intersected narrow grooves for the first heat pipe and interlaced channels for the second heat pipe. The results disclose that the special design of second heat pipe can improve the heat conduction in axial direction and enhance the capillary effect. Dung et al. [17] developed a capillary-driven two-phase flow model and further examined the influences caused by different micro-grooves, fluids, temperatures, radiuses and widths of groove. The study concluded that the triangular-microgroove has better influence of the liquid front position than semicircular-microgroove, and water has better influence of liquid front position than ethanol and benzene. Deng et al. [18] presented the capillary rise in copper micro V-grooves using two liquid acetone and ethanol. Micro V-grooves with deep and narrow profile, namely large aspect ratio, were found to be generally favorable to promote the capillary limit of grooved heat pipes. And he pointed out that micro V-grooves should be carefully designed to improve the heat transfer capacity, which in general should be of deep and narrow profile or large aspect ratio.

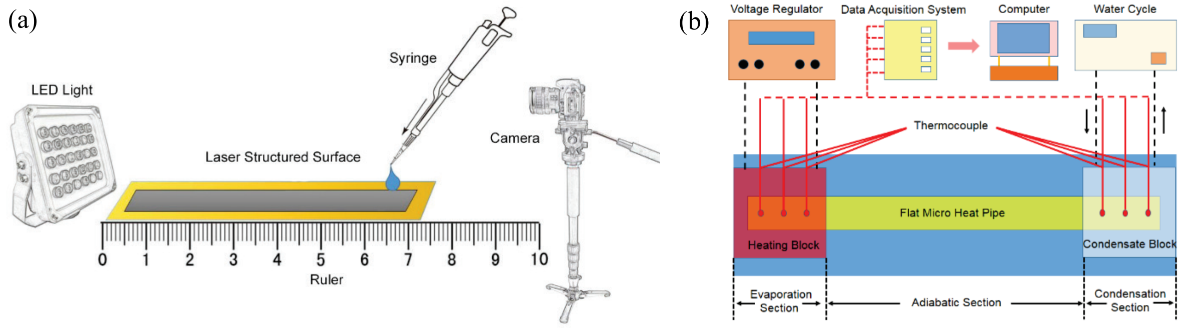

Fig. 1 (a) Schematic representation of droplet flow velocity measurement with 10 μL per injection, then camera was used to observe the spread of droplets. (b) Schematic representation of testing heat transfer performance. Voltage regulator was used to adjust different power to heat evaporation section. Thermocouples were used to measure the temperatures of evaporation section and condensation section, and collect them to data acquisition system.

In this paper, FMHP with microgrooves was processed in the copper substrate by 1064nm pulsed fiber laser. The influence of various laser processing parameters including pulse duration, scanning speed, scanning interval and the number of scanning cycles on the size and morphology of groove structures have been studied. The flow properties of droplets on the surface of groove structures with different aspect ratios were studied. In addition, the effects of groove wicks with different aspect ratio ranging from 0.5 to 2.5 on the heat transfer performance of FMHP were studied in detail.

2. Experimental

2.1 Materials

Copper substrate (99.9% purity) with a dimension of 10 mm × 100 mm × 3 mm was polished mechanically with the 800 and 1500 meshes SiC sandpapers respectively. Then it was cleaned ultrasonically in ethanol about 3 minutes, after that, it was taken out and dried it with compressed air before laser irradiation.

2.2 Experimental device and method

An IPG nanosecond laser source wavelength of 1064 nm, pulse repetition rate of 20 kHz ~ 500 kHz, and pulse duration 4 ns ~ 200 ns adjustable was used in the experiments. The focused diameter of the laser beam was approximately 30 μm. A two mirror galvanometric scanner with an objective lens (f = 100 mm) was used to focus and scan the laser beam in the horizontal direction. The laser scanning was performed line-by-line in the horizontal direction. After laser irradiation, the sample was cleaned ultrasonically with ethanol. Droplets were dropped on the surface with 10μL per injection. Then camera was used to observe the spread of droplets with LED light illuminating the substrate. The distance of the droplets flow at different time from the ruler can be seen clearly. Finally, the droplet flow velocity was measured as shown in Fig. 1a. Moreover, the method to test the heat transfer performance of FMHP was shown in Fig. 1b. Voltage regulator was used to adjust the heating power. The temperatures of evaporation section and condensation section were measured by thermocouples, and the data was collected to data acquisition system. According to temperature and heating power, the thermal resistance of FMHP can be obtained.

2.3 Determination of laser processing parameters

Processing parameters directly affect the morphology of the grooves. In order to explore the most suitable laser processing parameters for the fabrication of groove microstructures, the influence of various laser processing parameters including pulse duration, scanning speed, scanning interval, and number of scanning cycles on the size and morphology of micro grooves were studied, respectively.

2.4 Surface analysis

After laser irradiation, the copper surfaces with groove structure were created on pure copper substrate. The obtained structured surfaces were ultrasonically cleaned in ethanol for about 3 minutes to eliminate possible residues or contaminants. Then the samples were dried by compressive air for about 5 minutes. The morphology of the laser structured surfaces was studied by scanning electron microscopy (SEM, S-3400N-II, HITACHI Inc., Japan). The topography measurements were performed using a three-dimensional (3D) laser confocal microscope (OLS4000, OLYMPUS Inc., Japan).

3. Results and discussions

3.1 Laser structured surfaces

The microstructures are formed by the nanosecond laser ablation. When the laser beam irradiates on the material surface, surface thermal energy accumulates quickly and significant increases in the temperature of material surface. Depending on the magnitude of the temperature rise, various physical effects in the material include heating, melting, and vaporization of the material. Once the vaporization is initiated at the surface of the material, the continued laser

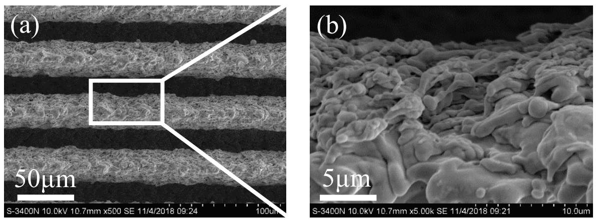

Fig. 2 SEM images of laser structured surfaces that were performed line-by-line in the horizontal direction. (a) SEM images of the surface with groove structure. (b) Corresponding high-magnification SEM image.

irradiation will cause the liquid–vapor interface to move inside the material. This is accompanied with the evaporative removal of material from the surface above the liquid–vapor interface. When the laser fluence is below the material's ablation threshold, no damage will be done to the material surface. However, when the laser fluence is close to the ablation threshold, the material surface begins to melt within the laser irradiated zone. Further increasing the laser fluence leads to precise material removal. The experiment is performed with a Gaussian beam, which has a higher energy at the center area of the circular spot than the edges. Hence, more material is ablated in the center of the laser beam scanned path, which resulting in the formation of groove structure and raised areas at the edge of the laser beam scanned path, as shown in Fig. 2a. The laser scanning is performed line-by-line in the horizontal direction. As a result, the laser irradiated surface was characterized with periodic arrays of grooves.

The topography of the groove structure changes greatly with different pulse duration. Pulse duration from 4ns to 200ns is selected respectively, as shown in Fig. 3. When the pulse duration is 100 ns, it is conducive to prepare high aspect ratio groove structure, as shown in Fig.3(c). According to the processing results of different pulse duration, we finally chose 100 ns as the best pulse duration to fabricate the groove structure. In a pulse duration of 100ns, surface

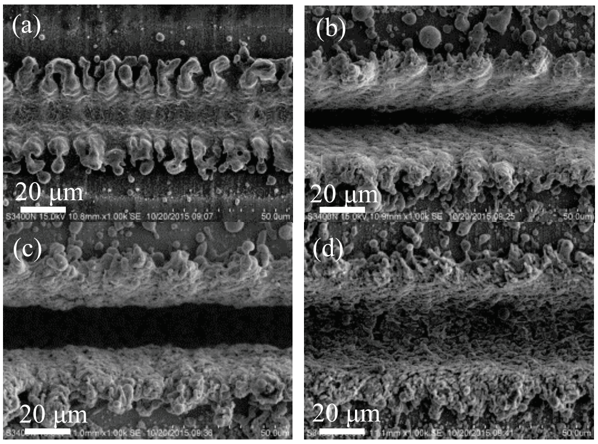

Fig. 3 Surface morphologies under different pulse duration. (a) 4ns, (b) 20ns, (c) 100ns, (d) 200ns.

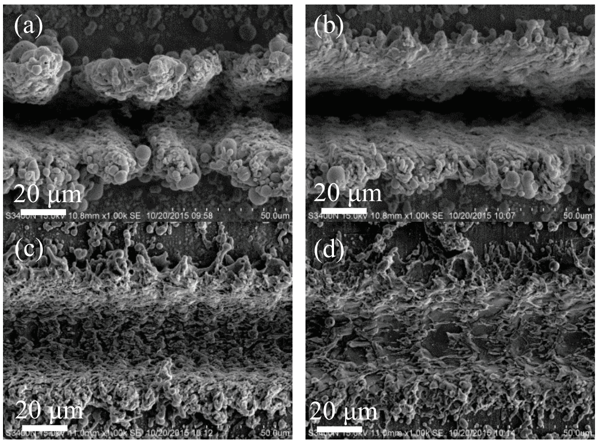

Fig. 4 Surface morphologies under different scanning speed at pulser duration of 100 ns. (a) 50 mm/s, (b) 100 mm/s, (c) 200 mm/s, (d) 500 mm/s.

topographies and morphologies under different scanning speeds are observed respectively, as shown in Fig. 4. When the scanning speed is 500 mm/s, the groove is very shallow. When the scanning speed is less than 100 mm/s, the re-solidification layer at the edge areas and inside the grooves are accumulated serious. So in comparison, the scanning speed of 200 mm/s is more suitable for processing high aspect ratio groove wick. Therefore, the follow-up experiments are all performed under conditions with pulse duration of 100 ns and scanning speed of 200 mm/s.

3.2 Effects of laser processing parameters on groove structures

3.2.1 Effects of scanning interval

To fabricate high aspect ratio groove wick, the effect of different scanning intervals on the topographies and morphologies of groove structure have been studied. When the scanning cycles is 4, scanning speed of 200 mm/s, pulse repetition rate of 40 kHz, pulse duration of 100 ns, four scanning intervals of 50, 60, 70, 80 μm are studied respectively. Fig. 5 shows the SEM and 3-D profile images of surface topographies and morphologies under different scanning interval. Fig. 5(a1) shows that when the scanning interval is 50 μm, the re-solidification layers is accumulated at the edge area and integrate together with grooves. As the scanning interval increases, re-solidification layer gradually separate and finally accumulate at the edge area but cannot join together, this makes part of the surface blank (Fig. 5(d1)). As shown in Fig. 5(a4), the period of these grooves is 50 μm which is similar to the interval of the adjacent laser scanning lines, and the average depths of the groove is about 90 μm. When the scanning interval is 60 μm, the re-solidification layer can't fully join together. There are some micro-holes exist in the re-solidification layer as shown in Fig. 5(b2). However, as the scanning interval increases to 70 μm and 80 μm, the re-solidification layer on the top of grooves gradually begins to separate, and finally achieves complete separation. The reason is that the laser fluence used in the experiment is much higher than the copper removal threshold. At this time, the material removal mode is mainly dominated by evaporation. The material removed is ejected in an explosive manner. Due to limited eruption distance, as the scanning interval increases, the re-solidification layer cannot integrate together and finally form the morphology like Fig. 5(c2, d2). The average depth of the groove has some decline tendency as shown in Fig. 5(c4, d4). It can be seen that, by simply changing the scanning interval of the laser beam, the topography of the groove is tuned precisely. To get more effective number of grooves with high aspect ratio, the most suitable scanning interval is 50 μm.

3.2.2 Effects of scanning cycles

From Fig. 5(d1), when the number of scanning cycles is 4, the average depth of the groove is 85 μm. Fig. 6 shows the SEM and 3-D profile images of groove structure fabricated with different number of scanning cycles. Four groups of scanning cycles of 1, 6, 8, and 10 are selected at the scanning interval of 50 μm, scanning speed of 200 mm/s, pulse repetition rate of 40 kHz and pulse duration of 100 ns. SEM images showed that the accumulation situation of re-solidification layer at the edge areas is similar,

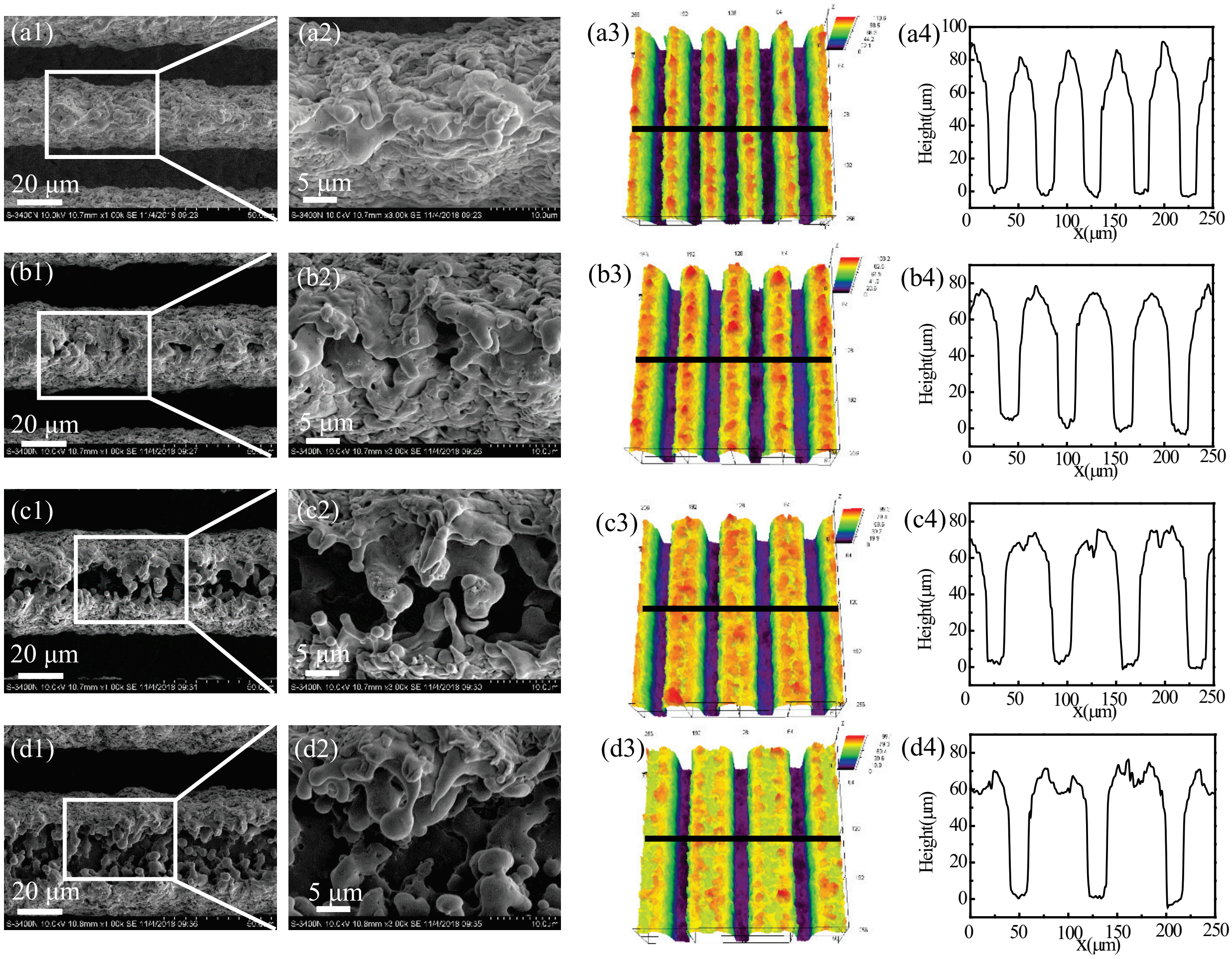

Fig. 5 Surface topographies and morphologies under different scanning interval, scanning cycles of 4, scanning speed of 200 mm/s, pulse repetition rate of 40 kHz, pulse duration of 100 ns. (a1-d1) SEM images of the surface with groove structure which were corresponding to different scanning interval of 50 µm, 60 µm, 70 µm, and 80 µm. (a2-d2) Corresponding high-magnification SEM images. (a3-d3) Surface 3D height map obtained by the 3D laser microscope. The black lines show the corresponding areas for the topography measurement as shown in a4−d4. (a4−d4) Corresponding surface profiles.

no matter how the number of scanning cycle is. Fig. 6(a4−d4) shows the average depth of groove structure fabricated with different number of scanning cycles. When the number of scanning cycles increases from 1 to 8, the average depth of groove structure presents an increase tendency. In particular, when the scanning cycles is 8, the average depth of groove reaches to the maximum of 125 µm. And at this time, the groove has the largest aspect ratio of 2.5. When the number of scanning cycle is greater than 8 for 10, the average depth of groove structure presents a saturated tendency. The groove copper surfaces are fabricated by repeating scanning sequences, and the surface material is removed by the laser ablation. When the number of scanning cycles increases, the energy density absorbed by the surface material increased also, inducing more re-melting of the surface structures. The debris was finally cooled to form thick re-solidification layer on the copper surface. As the scanning cycle continues to increase, the former re-solidification layer is melted again, which results the re-solidification layer is accumulated inside the grooves as shown in Fig. 6(d3). As the number of scanning cycles continues to increase, the accumulation of re-solidification layer became more serious, which is not conducive to the flow of droplets in the grooves. In summary, the best number of scanning cycle is 8. Under this circumstance, the average depth of groove reaches to the maximum of 125 µm and corresponding aspect ratio of the groove wick is 2.5.

3.3 Comparison of droplet flow velocity

The droplet flow velocity has great influence on the heat transfer performance of the heat pipe. From the working principle of heat pipe we can know that the faster the droplet flow velocity, the greater the amounts of heat transfer in the same time. Four groups of scanning cycles of 2, 4, 6, and 8 are selected to create the groove structures with the aspect ratios of 1.0, 1.8, 2.2 and 2.5 respectively. After laser irradiation, the samples are cleaned ultrasonically with ethanol for 3 minutes to remove impurities on the surface. The size of the laser structured area is 15 mm × 40 mm. As shown in Fig. 7, the red line corresponded to the position of droplet at 0.5 second and 1 second respectively. It can be inferred that with the increasing of aspect ratio, the average flow velocity of droplet on the groove surface has an increasing trend before 0.5 second. But when the aspect ratio

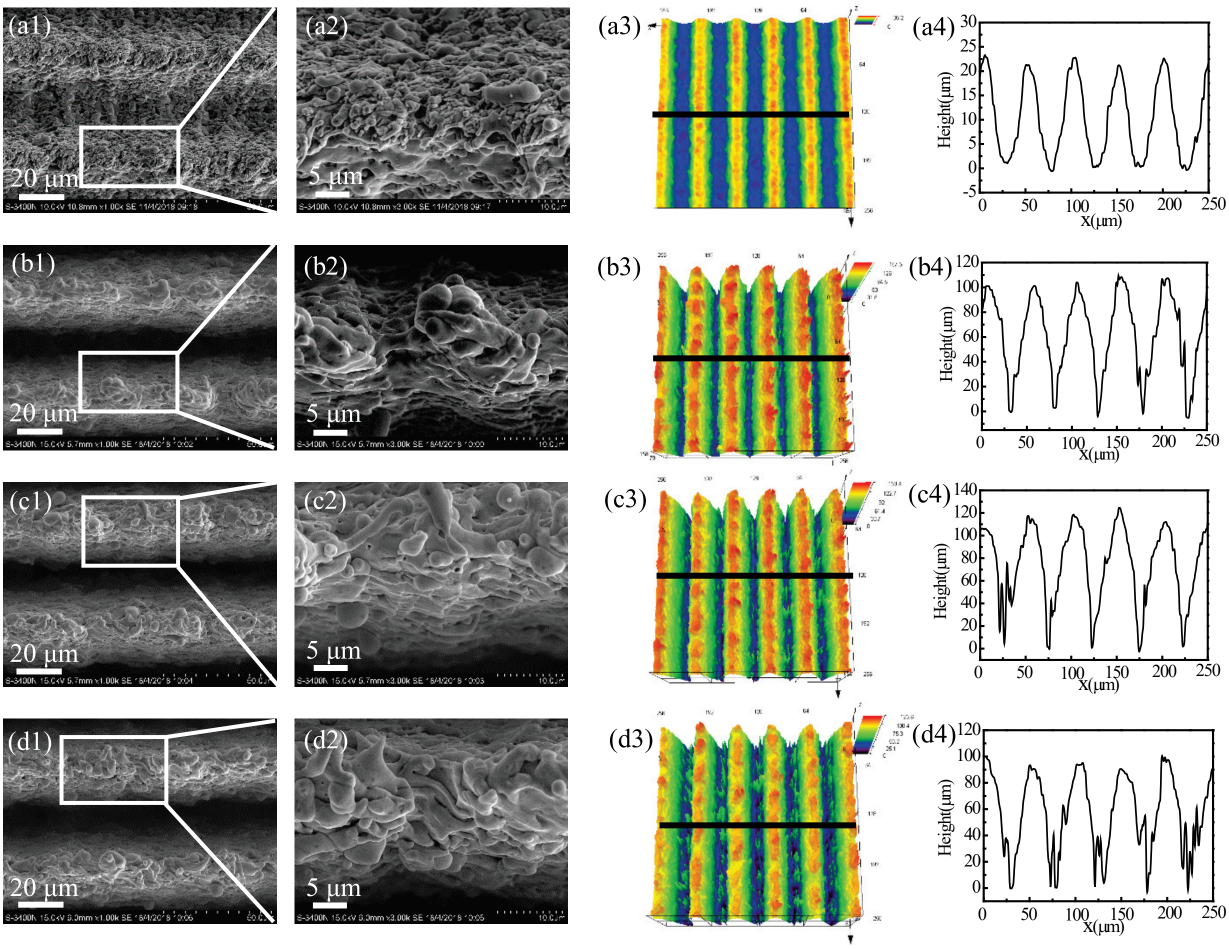

Fig. 6 Surface topographies and morphologies fabricated with different number of scanning cycles, scanning interval of 50 μm, scanning speed of 200 mm/s, pulse repetition rate of 40 kHz, pulse duration of 100ns. (a1-d1) SEM images of the surface with groove structure which were corresponding to different number of scanning cycles of 1, 6, 8, and 10. (a2-d2) Corresponding high-magnification SEM images. (a3-d3) Surface 3D height map obtained by the 3D laser microscope. The black lines show the corresponding areas for the topography measurement as shown in a4−d4. (a4−d4) Corresponding surface profiles.

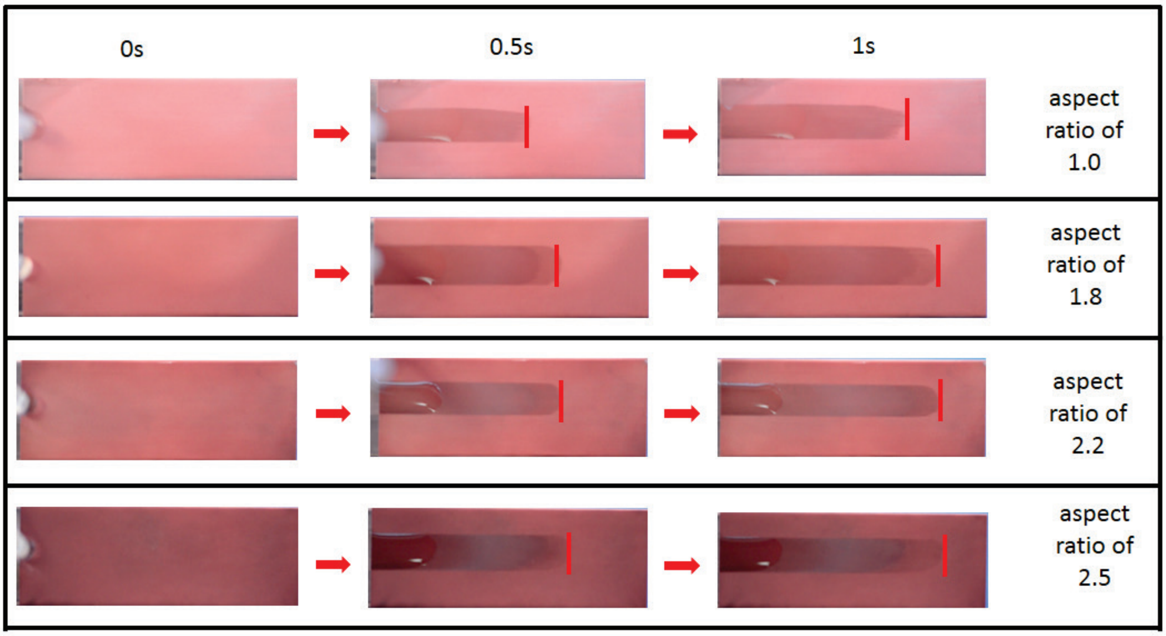

Fig. 7 Comparison of flow velocity of droplet in the groove surface with different aspect ratio. Four aspect ratios of 1.0, 1.8, 2.2 and 2.5 are fabricated on the 15 mm × 40 mm area. The volume of droplet was 10 μL. The red line corresponded to the position of droplet at 0.5 second and 1 second, respectively.

was greater than 1.8, the average droplet flow velocity tended to be the same over time. As the picture shows at time of 1 second, the average droplet flow velocity is almost the same. The main factor affecting the droplet flow velocity is capillary force, which is determined by the aspect ratio of the grooves. Capillary driving force of V-groove was analyzed in more detail by Rye et al. [19], as shown in Eq. 1.

$$F = \frac{2\gamma h_0}{\sin\alpha}[\cos\theta - \cos\alpha] \quad (1)$$

Where F is the capillary driving force, α is related to the groove angle, θ is the contact angle, γ is the liquid surface tension, and h_0 is the groove depth (Fig. 8). It can be known from the formula, with the increase of α, namely, the greater the aspect ratio, the greater the capillary force provided by the groove structure. As shown in Fig. 7, before 0.5 second, the droplet has faster flow velocity on the groove surface with higher aspect ratio. This is consistent with the theoretical situation. However, as the aspect ratio increases, the frictional resistance of the inner wall of the groove to the liquid droplets also increases, which results in the droplet flow velocity not continuing to increase with the increase of the aspect ratio. Finally, the average droplet flow velocity tends to be the same over time. Even so, the groove with a large aspect ratio can drive more droplets at the same time, which further improves the heat transfer performance of the heat pipe.

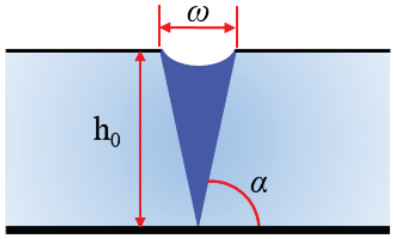

Fig. 8 A schematic drawing of V-groove profile.

3.4 Heat transfer characteristics

The thermal performance of the flat micro heat pipe (FMHP) in the horizontal orientation has been evaluated under room temperature. A 15 mm × 15 mm copper heater is attached to the lower surface of the evaporation section. In the same way, a 15 mm × 15 mm copper cooler is attached to the lower surface of the condensation section with circulating cooling water. There are thermocouple attached to the evaporation section and condensation section to measure its temperature. The thermal resistance can be obtained through temperature difference of evaporation section and condensation section and the input power. In the experiment, thermal resistance of FMHP with different aspect ratio groove wick is measured respectively. With the increase of input power, the overall thermal resistance presents a decline tendency. However, under the same condition, the FMHP with higher aspect ratio groove wick has a lower thermal resistance. When the number of scanning cycles was 8, the aspect ratio of groove wick reaches the maximum value of 2.5, as shown in Fig. 9(a, b). Correspondingly, the FMHP with groove wick of this type has a better heat transfer property, the minimum thermal resistance is 0.038 °C / W, and the maximum power of heat transfer is 15 W, as shown in Fig. 9c. It indicates that aspect ratio is an important factor to affect the heat transfer performance of FMHP with groove wick.

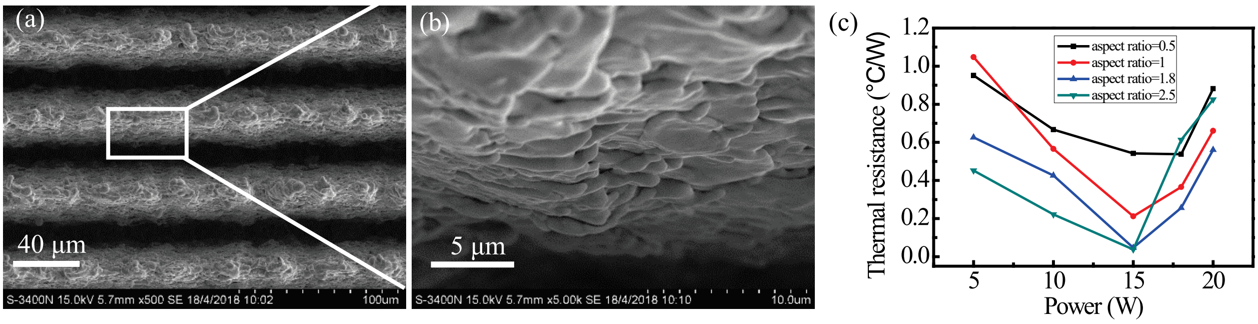

Fig. 9 Pulsed fiber laser fabricated surface with groove microstructures and heat transfer curve of FMHP. (Scanning speed of 200 mm/s, pulse duration of 100ns, pulse repetition rate of 40 kHz, scanning interval of 50 μm, and scanning cycles of 8). (a) SEM image of the laser structured groove wick; (b) High magnification SEM image shows that the inner wall of the groove is smooth; (c) Thermal resistance under different input power.

4. Conclusion

In this study, a pulsed fiber laser is proposed to process groove wick on copper substrate with the periods of 50 μm and depth of 125 μm. A series of groove structures are fabricated to explore the effects of processing parameters on the formation. The groove structures can be steadily formed when the pulse duration is 100 ns and scanning speed is 200 mm/s. Moreover, the scanning interval directly determined the periods of these grooves. The groove structure is densest when the scanning interval is 50 μm, the re-solidification layer is accumulated at the edge area and integrate together with grooves. A distinct increase of the average depth of grooves can be observed with the number of scanning cycles increasing. When the number of scanning cycles is 8, the average depth of grooves is around 125 μm, the aspect ratio of groove wick is approximately 2.5. The FMHP with the groove wick of this type has a better heat transfer property, the minimum thermal resistance is 0.038 °C / W, and the maximum input power is 15 Watts.

Acknowledgments

Financial assistance for this work is granted by the National Key Research and Development Program of China (2018YFB1107700), the National Natural Science Foundation of China (51575114 and 51805093) and the Guangzhou Science and Technology Project (201607010156).

References

[1] M.K. Yim, K.M. Lee, and T.H. Han: IEICE Electronics Express, 11, (2014) 20140944:1-6.
[2] S. Sharifi, and T.S. Rosing: IEEE. T. Comput. Aid. D, 29, (2010) 1586.
[3] P. H. Chen, S.W. Chang, K. F. Chiang, and J. Li: Recent Patents on Engineering, 2, (2008) 174.
[4] L. Lv, and J. Li: Appl. Therm. Eng, 122, (2017) 593.
[5] M. Khalili, and M.B Shafii: Appl. Therm. Eng, 94, (2016) 59.
[6] D. Jafari, H. Shamsi, S. Filippeschi, P.D. Marco, and A. Francoa: Exp. Therm. Fluid. Sci, 84, (2017) 120.
[7] Y. Tang, H. Tang, J. Li, S.W. Zhang, B.S. Zhuang, and Y.L. Sun: Appl. Therm. Eng, 115, (2017) 1020.
[8] J. Zeng, L. Lin, Y. Tang, Y.L. Sun, and W. Yuan: Int. J. Heat. Mass. Tran, 104, (2017) 918.
[9] Zeng J, Zhang S, Chen G, L. Lin Y.L. Sun, L. Chuai, and W. Yuan: Appl. Therm. Eng, 130, (2017) 185.
[10] Y.T. Chen, S.W, Kang, Y.H. Hung, C.H. Huang, and K.C. Chien: Appl. Therm. Eng, 51, (2013) 864.
[11] X. Wang, Y. Tang, and P. Chen: Energ. Convers. Manage, 50, (2009) 1384.
[12] Y. Tang, P. Chen, and X. Wang: Energ. Convers. Manage, 51, (2010) 1849.
[13] X.Z. Xie, Q. Weng, Z.Q. Luo, J.Y. Long, and X. Wei: Int. J. Heat. Mass. Tran, 125, (2018) 658.
[14] C. Sun, X.W. Zhao, Y.H. Han, and Z. Gu: Thin. Solid. Films, 516, (2008) 4059.
[15] X.B. Li, X.L. Liu, Z.M. Shi, H. Jiang, X.Z. Lou, S. G. Wang, G. Han, and Y.G. Pan: ICICTA & Automation IEEE Computer Society, Zhangjiajie, Hunan, (2012) 614.
[16] C. Wang, Z.L. Liu, G.M. Zhang, and M. Zhang: Exp. Therm. Fluid. Sci, 48, (2013) 222.
[17] N. Dung, F.S. Chuang, and K.J. Wang: Continuum. Mech. Therm, 26, (2014) 423.
[18] D.X. Deng, Y. Tang, J. Zeng, S. Yang, and H.R. Shao: Int. J. Heat. Mass. Tran, 77, (2014) 311.
[19] R.R. Rye, J.A. Mann, and F.G. Yost: Langmuir, 12, (1996) 555.

(Received: June 23, 2018, Accepted: February 17, 2019)